Electrically Tunable Bandpass Filter with Narrow Bandwidth of 27 nm

Ramesh Manda,[1] Srinivas Pagidi,[1] Yunjin Heo,[1] Sub Shin Hoon,[1,2] Hong Gwon Lee,[1] Hyoung Soo Park,[1] Daun Mun,[1] Young Jin Lim,[1] Seung Hee Lee[1*]

[1]Applied Materials Institute for BIN Convergence, Department of BIN Convergence Technology and Department of Polymer-Nanoscience and Technology, Jeonbuk National University, Jeonju 54896, Republic of Korea, [2]LG Display Co., Ltd., Gumi, Gyungbuk, 730-350, Korea

E-mail: lsh1@jbnu.ac.kr

Abstract

We propose an electrically tunable narrow bandwidth bandpass filter in which the band gap of polymer stabilized blue phase liquid crystal (PS-BPLC) with distinct crystallographic orientations can be tuned on electric field sweeps from red to blue with a narrow bandwidth (27 nm). Owing to the narrow bandwidth which can cut specific wavelength, it could be used as a filter to enhance color gamut in LCDs. In addition, the proposed bandpass filter exhibits much wider viewing angle property than Cholesteric LC bandpass filter.

Keywords

Blue phase liquid crystal; bandpass filter; color gamut; viewing angle.

1. Introduction

The tunable color filter has drawn much attention due to their potential applications in display and telecommunication. However, due to wider bandwidth, the crosstalk between the primary colors occurs that deteriorates the display quality and device performance. Recently, the tunable photonic band gap material, like BPLC/PS-BPLC, has been proposed for tunable color filters for improving the display [1,2]. BPLC is typically formed through self-assembly of LC molecules into DTC those at which possesses a cubic symmetry with lattice constant few 100's of nanometer and exhibits a photonic band gap effect. The BPLC are also well-known for their great advantageous of easy processing, fast response, and optically isotropic phase [3,4,5]. Although the BPLC is having a great advantage of band gap tuning which can be utilized for color filter applications, the shorter operating range and unwanted multiple reflections due to intrinsic platelets deteriorates the device performance [6,7].

Here, we demonstrate a narrow bandwidth bandpass filter utilizing a field-induced band gap of monodomain PS-BPLC. The proposed bandpass filter is exhibiting a wider tuning range, 241 nm, and a narrow bandwidth, 27 nm. Precisely oriented distinct cubic lattices are resulted in a narrow bandwidth reflection, thus reduces the crosstalk between three primary colors red green, and blue. Owing to the narrow bandwidth and wider band gap range, the proposed device is exhibiting 82% of NTSC color gamut in CIE1931 color space. Further, this bandpass filter shows a wide viewing angle property such that the filtering capability is kept in wide angles.

2. Materials and Experimental Procedure

A high HTP chiral dopant, SRM17, is dispersed into a high dielectric anisotropic positive nematic LC, MLC2053, to form a BPLC. The structure of the BP is stabilized by the combination of the mosegenic and non-mesogenic monomers, RM257 and TMPTA, respectively, and a chiral monomer, SRM03. The TMPTA is usually stabilizes the disclination cores whereas the RM257 which exhibits a nematic LC phase in the operated temperature is mostly occupies inside the DTCs. We particularly emphasize that the chiral monomer and portion of the mesogenic monomer polymerizes inside the DTC. The alterations of polymer network formation in both conventional PS-BPLC and the PS-BPLC stabilized by chiral monomer and mesogenic monomer is depicted shown in **Figure 1**. Sample S1: MLC2015 (84 wt.%), SRM17 (1.1 wt.%), and SRM03 (5.9 wt.%); S2: MLC2015 (81.2 wt.%), SRM17 (1.4 wt.%), and SRM03 (8.4 wt.%); S3: MLC2015 (80 wt.%), SRM17 (1.8 wt.%), and SRM03 (9.2 wt.%). We have added 7 wt% of RM257 and 1 wt% of TMPTA to the BPLC. A small amount of photo-initiator, 1 wt% of Irgacure907, is added to every sample to initiate the polymerization.

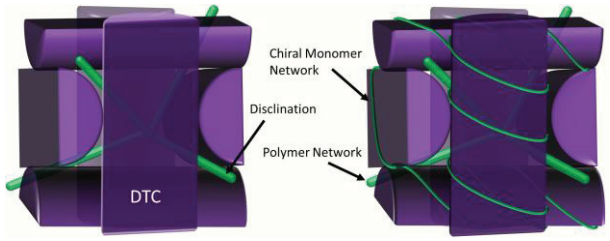

Figure 1. Polymer network formation in PS-BPLC stabilized by a conventional approach (first) and proposed model (second).

The experimental cell consists of uniform indium-tin-oxide (ITO) coated substrates. To achieve a monodomain BP, the glass substrates were coated with polyimide (AL16301, JSR Micro Korea) and unidirectionally rubbed with velvet cloth. Thereafter, the two substrates are attached in anti-parallel direction. The cell gap was fixed to 7 μm. A homogeneous mixture of BPLC and monomers was infiltrated into the cell at 92 °C and subsequent observations were carried out with polarizing optical microscope (POM) (Nikon eclipse, E600 POL). The temperature of the sample was accurately maintained at cooling rate 0.3 °C/min. The polymerization was performed by illuminating with 20 mW/cm^2 intensity UV light for 10 min at BPI phase. After essential characterizations of BPLC phase, the field dependent characterizations were performed under crossed polarizer's by applying 1 kHz square-wave voltage supplied by the function generator (Tektronix, AFG3101C) and modulated by an amplifier (FLC Electronics, A400). The Bragg reflection spectrum was measured by a reflection spectrometer (Ocean Optics, USB2000+) connected to POM.

3. Results and Discussion

Firstly, we identify the BP phase with POM and compared the phase before and after polymerization to estimate the phase range. The POM textures shown in **Figure 2** are evident of the BPLC formation between isotropic (absence of photonic effect) and cholesteric phase (wide reflection colors). It is apparent from POM textures a quite uniform and clearly distinguishable monocolor single domain is formed, which is evident of unidirectional orientation of cubic lattices in a large scale. The

 ISSN 0097-996X/20/4803-1930-$1.00

tendency to holding cubic lattice crystals in a particular direction is governed by the surface anchoring of the polyimide. The monodomain BP phase starts appearing at ~84.5 ºC for all the samples and ends at 67.7 ºC, 69.5 ºC, and 63.8 ºC for S1, S2, and S3, respectively. The BPII phase exists in a short range, <2 ºC whereas the BPI phase appears in the range of 16.8 ºC, 13.1 ºC, and 20.6 ºC for S1, S2, and S3, respectively. The BPII phase exists in a very narrow temperature range and exhibits a wider bandwidth reflection with less color saturation compared to BPI phase. More clearly, the BPI phase is exhibiting vivid colors, red (S1), green (S2), and blue (S3) in a wide temperature range, indicating manipulation of polymer network formed inside the DTC by a chiral monomer has a huge impact on the Bragg reflection. The difference between temperature range in BPI and BPII may arise from the difference in spatial arrangements of disclinations where all the disclinations join in BPII while non-intersected disclinations in BPI. However, the tunable reflection color from red to blue by carefully manipulating concentration of both the chiral dopant and chiral monomer was achieved.

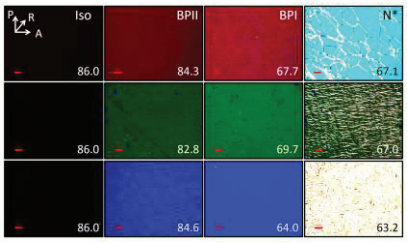

Figure 2. Temperature dependent POM textures of monodomain BPLC. S1 (top row), S2 (middle row), and S3 (bottom row).

As a next step, we measure the temperature dependent Bragg reflection wavelength (λ_B) to find out the exact reflection wavelength and its temperature dependency of LC textures. The Bragg reflection measurements of monodomain BPLC exhibits clearly distinguishable single narrow reflection peak with peak wavelengths at 70 ºC are 649 nm, 519 nm, and 433 nm for S1, S2, and S3, respectively. Further, we have calculated the bandwidth of each reflection peak defined as the full width at half maximum (FWHM). The calculated bandwidth is 25.1 nm, 25.4 nm, and 26.3 nm for S1, S2, and S3, respectively, for BPI phase. The obtained bandwidth is narrow.

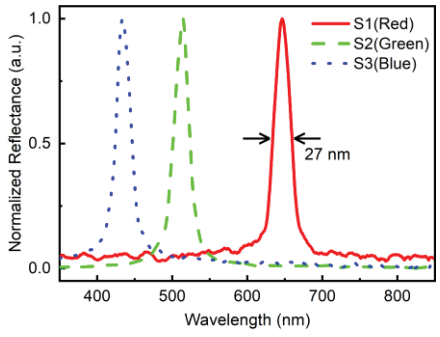

Figure 3. Bragg reflection peak of monodomain BPLC.

Further, to see more insight into chiral monomer influence on the reflection wavelength, we find out particular cubic planes associated with Bragg reflection of each sample. The incident light encounters a set of reflection plane those are aligned parallel to the propagation direction of the incident light. We also found that, from Wedge cell measurements, the reflection peak of sample S1 is originated from (110) cubic plane. In other words, all (110) cubic planes align parallel to the substrate's normal. Similarly, the reflection peak of sample S2 and S3 are originated from (200) and (211) cubic planes, respectively.

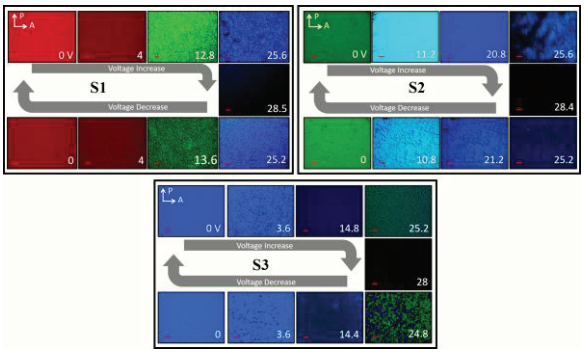

Figure 4. The field dependent POM textures of S1, S2, and S3.

When the phase is addressed to the external electric field, we found that the monodomain BPLC is not only manipulated by the chiral monomer concentration but also controlled by the electric field. It is evident that the sample exhibits vivid colors on field increase, as shown in **Figure 4**. It is interesting to note that the electrically tunable reflection wavelength correspond to vivid colors was obtained on field increase and field decrease as well. As voltage increase, the reflection wavelength linearly shifts from the red color to green color and then blue color for S1. The phase appears as black at higher field due to reflection peak shifted to UV region. We remarkable achieved the total reflection wavelength tuning in the spectral range of 240 nm, by applying the field ~29 V, which is wider than that of reported elsewhere [6-8]. On the other hand, the S2 and S3 shows the blue shift and green shift at spectral range of 95 nm and 80 nm, respectively. We particularly emphasize that the sample S1 is capable of tuning the band gap covering most of the visible spectra starting from red to blue wavelengths. When the field is applied along the particular direction of the cubic lattice, the electric torque causes finite lattice distortion such as either lattice expansion or lattice shrinkage; thereby incident light encounters different sequential planes of the cubic lattice. In the present BPLC system, relatively less concentration of the monomer, which forms the polymer network in the disclinations, with compare to polymer network formed inside the DTC, allows a finite lattice deformation due to electrostriction under strong applied field. It is worth to mention that the cubic lattice deformation due to electrostriction is completely recoverable, which is not usual phenomenon in the conventional polymer stabilized BPLC. The strong coupling of LC molecules with polymer network might be the reason for lattice distortion recovery. Another interesting point to notice that the peak wavelength of S1 and S2 takes different trend with compare to the S1. This alteration could be attributed from the field acting along the four-fold symmetric axis. The average bandwidth is 29 nm, 27 nm, and 32 nm on field increase and 32 nm, 31 nm, and 29 nm on field decrease for S1, S2, and S3, respectively. Totally, the obtained bandwidth is quit narrow all over the driving range upon field increase and decrease as well.

The measured band gap hysteresis is considerably smaller that was defined as the band gap difference between the increase and decrease voltage sweeps. More specifically, the

band gap hysteresis is smaller than 10 nm for samples S2 and S3 while it is <20 nm for S1. The achieved hysteresis is relatively smaller by comparing it with similar literature where it is either huge or required special treatment [6,9,10]. It implies that the lattice distortion induced by the electric field was mostly recovered like field-induced refractive index. In our device, the polymer network formed inside the DTC provides enough anchoring energy due to the proximity of LC molecules with polymer backbone. In addition, the polymer network formed inside the DTC is strong enough to sustain the distortion due to external field whereas it is not true for polymer network formed by monomers in disclination lines.

In order to evaluate the quantity of the color, we measured the chromaticity of prepared monodomain samples as a function of applied voltage. Here, the color values are measured for each color of POM image based on the International Commission on Illumination (CIE) 1931 color space chromaticity diagram. The color values are converted to chromatic coordinates by using standardized conversion equations defined by the CIE special commission [11,12]. The color coordinates of S1 is covering a wider area in the color space while S1 and S2 covers a narrow area, **Fig. 6**. More specifically, the chromaticity coordinates of the sample S1 starts from the red region (0.62, 0.24) and shifted to the green region (0.28, 0.68) by applying 12.8 V, and then shifted to the blue region (0.18, 0.10) for 29V. The chromatic coordinates of sample S2 starts from the green region (0.27, 0.69) and linearly shifted to the blue region (0.20, 0.19) whereas the sample S3 is started at the blue region (0.18, 0.14) and shifted to the green region (0.22, 0.37) for 29 V, respectively. An inbuilt halogen lamp with 100 W power (HLX 64623, OSRAM) was employed for obtaining POM textures. However, the sample S1 is potential to show three primary color coordinates of red, blue, and green in the color space. Totally, the sample S1 exhibits 85% of color gamut in the NTSC (National Television System Committee) color space. Further increase of color gamut could be presumed by replacing the halogen lamp with a blue LED.

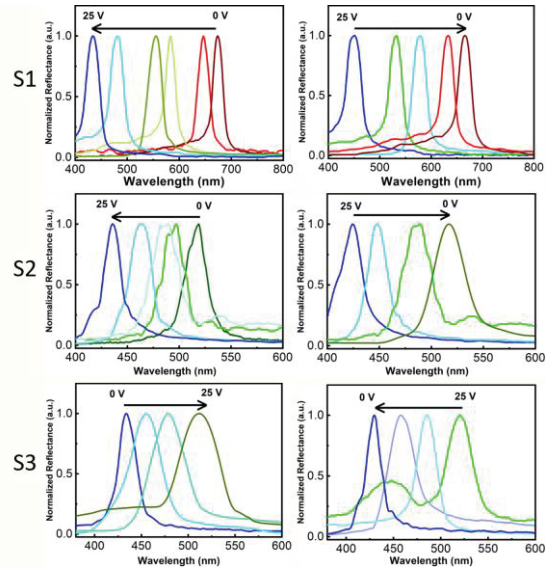

Figure 5. The electric field induced Bragg reflection peak shift. Filed increase (first column) and field decrease (second column).

Afterward, we examine the efficiency of transmitted light for this monodomain BPLC for selective polarization of incident light. Since the BPLC is featured by the highly twisted local director structures, the incident direction of the linearly polarized light is set to unchanged. Quantitative results were extracted by comparing with transmission spectra at the isotropic phase (above T_{NI}). The obtained data, shown in **Fig. 6(b)**, reveals that we achieved ~50% of transmission efficiency for all the samples. In addition, there is almost no overlap between the reflection peaks of corresponding red, blue and green colors. The narrow bandwidth that could decrease the potential crosstalk between primary colors and a single reflection peak, which indicates a distinct color of the sample, enables this device as a potential candidate for tunable color filters. The fast response time, ~350 ms, is another benefit for this device, which opens new prospects.

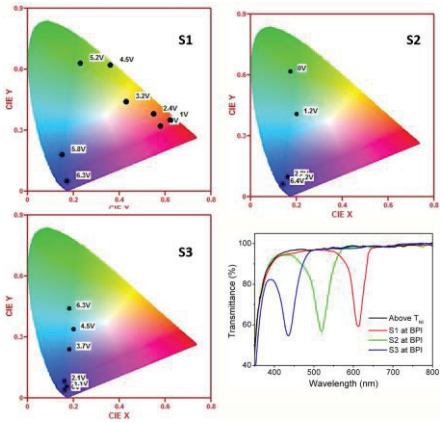

Figure 6. (a) Measured chromatic coordinates in CIE 1931 color space. (b) The transmission spectra of samples with incident linearly polarized light.

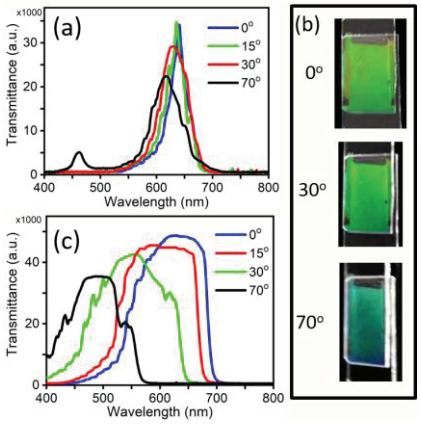

Figure 7. Viewing angle-dependent reflection spectra of S1 (a). Photographic images of S2 (b). Reflection spectra of conventional ChLC (c).

Next, we have measured the viewing angle-dependent reflection spectra for S1 with different incident light directions of 0°, 15°, 30°, and 70°. Quantitative results are compared with the conventional cholesteric phase. The angle is made by tilting the sample on the POM stage and subsequent reflection spectrum is recorded. As shown in **Fig. 7(a)**, the Bragg reflection spectrum is not evident of much change in either peak wavelength or bandwidth up to 30° of sample tilt. However, the tilt angle at 70° is exhibiting small variations such as a slight

increase in bandwidth and band gap shift toward lower wavelengths. In addition, the intensity of peak also tends to decrease and blue color appears. However, the reflection peak shift is relatively smaller with compare to the conventional cholesteric LC has shown in **Fig. 7(c)**. The manifestation of the blue color peak is originated from the different planes in the cubic lattice. The photographic images of S2 with respect to the tilt angle as shown in **Fig. 7(b)**. The phase shows a reasonable wider viewing and still possesses an optically isotropic cubic structure.

4. Impact

We propose an electrically tunable narrow bandwidth bandpass filter. The reflection band gap originated from a homogeneously aligned cubic lattice of monodomain PS-BPLC is utilized as bandpass filter. A narrow bandwidth reflection, 27 nm, is emerged from a precisely organized cubic lattice, which eliminates the unwanted colors and reduces the crosstalk between the three primary colors of red, green, and blue. It utilizes the advantage of narrow bandwidth reflection of distinct cubic lattice and exhibiting 85% of NTSC color gamut in CIE1937 color space. The filter exhibits much wider viewing angle property than the cholesteric bandpass filter. The proposed bandpass filter potential to use not only for LCDs color filters but also for photonic circuits and telecommunications applications.

5. Acknowledgement

This research was supported by the Basic Science Research Program through the National Research Foundation of Korea (NRF) grant number (2016R1D1A1B01007189) and (2019R1A5A8080326).

6. References

1. Lin JD, Wang TY, Mo TS, Huang SY, Lee CR. Wide-band spatially tunable photonic bandgap in visible spectral range and laser based on a polymer stabilized blue phase. Scientific Reports. 2016, 6:30407.
2. Chen CW, Li CC, Jau HC, Yu LC, Hong CL, Guo DY, Wang CT, Lin TH. Electric field-driven shifting and expansion of photonic band gaps in 3D liquid photonic crystals. ACS Photonics. 2015, 2(11):1524-31.
3. Lee H, Park HJ, Kwon OJ, Yun SJ, Park JH, Hong S, Shin ST. The world's first blue phase liquid crystal display. In SID Symposium Digest of Technical Papers. 2011, 42(1):121-124.
4. Chen KM, Gauza S, Xianyu H, Wu ST. Submillisecond gray-level response time of a polymer-stabilized blue-phase liquid crystal. Journal of display technology. 2010, 6(2):49-51.
5. Heppke G, Jerome B, Kitzerow HS, Pieranski P. Electrostriction of the cholesteric blue phases BPI and BPII in mixtures with positive dielectric anisotropy. Journal de Physique. 1989, 50(19):2991-2998.
6. Chen CW, Hou CT, Li CC, Jau HC, Wang CT, Hong CL, Guo DY, Wang CY, Chiang SP, Bunning TJ, Khoo IC. Large three-dimensional photonic crystals based on monocrystalline liquid crystal blue phases. Nature Communications. 2017, 8(1):727.
7. Lu SY, Chien LC. Electrically switched color with polymer-stabilized blue-phase liquid crystals. Optics Letters. 2010, 35(4):562-564.
8. Sridurai V, Mathews M, Yelamaggad CV, Nair GG. Electrically tunable soft photonic gel formed by blue phase liquid Crystal for switchable color-reflecting mirror. ACS applied materials & interfaces. 2017, 9(45):39569-39575.
9. Lin TH, Li Y, Wang CT, Jau HC, Chen CW, Li CC, Bisoyi HK, Bunning TJ, Li Q. Red, green and blue reflections enabled in an optically tunable self-organized 3D cubic nanostructured thin film. Advanced Materials. 2013, 25(36):5050-5054.
10. Liu HY, Wang CT, Hsu CY, Lin TH, Liu JH. Optically tuneable blue phase photonic band gaps. Applied Physics Letters. 2010, 96(12):121103.
11. Lin P, Cong Y, Sun C, Zhang B. Non-covalent modification of reduced graphene oxide by a chiral liquid crystalline surfactant. Nanoscale. 2016, 8(4):2403-2411.
12. Fairman HS, Brill MH, Hemmendinger H. How the CIE 1931 color-matching functions were derived from Wright-Guild data. Color Research & Application. 1997, 22(1):11-23.